

Aqueous Supramolecular Polymer Formed from an Amphiphilic Perylene Derivative**

Alix Arnaud, Joël Belleney, François Boué, Laurent Bouteiller, Géraldine Carrot, and Véronique Wintgens*

Supramolecular polymers are reversible one-dimensional assemblies that are formed by dynamic noncovalent intermolecular interactions.^[1] With the exception of biological systems, such self-assemblies are mostly formed in organic and nonpolar solvents and rely on hydrogen-bonding or metal–ligand interactions. Interesting material properties have been demonstrated in the case of specific monomers, such as ureidopyrimidones^[2] and bisureas,^[3] which can self-organize in very long chains. These materials combine the properties of conventional polymers with reversibility and responsiveness. It is a challenging objective to expand this innovative theme to aqueous media. The main drawback of relying on hydrogen bonds is their limited strength in polar solvents, particularly in water; therefore, other noncovalent interactions should be considered for aqueous media. So far, only a few synthetic supramolecular polymers have been prepared in water, and most have relied on aromatic and/or hydrophobic interactions.^[4–7] Moreover, their syntheses are not well-suited for large-scale preparation and their properties as materials (such as rheology) have never been reported. We thus designed amphiphilic perylene derivative **1** which contains a large hydrophobic aromatic core surrounded by four hydrophilic arms and which can be prepared on a large scale by an easy synthetic route with facile purification (Scheme 1). Such a design should provide a one-dimensional assembly in water through intermolecular π -stacking and/or hydrophobic interactions. The four hydrophilic arms are expected to hinder the possible aggregation of such assemblies and to ensure their water solubility. Herein, we detail the synthesis and the characterization of the supramolecular polymer formed by the association of monomer **1** in water.

[*] Dr. A. Arnaud, J. Belleney, Dr. L. Bouteiller
Laboratoire de Chimie des Polymères, UMR 7610
Université Pierre et Marie Curie
4, place Jussieu, 75252 Paris cedex 05 (France)
Fax: (+33) 1-4427-7089
E-mail: bouteil@ccr.jussieu.fr

Dr. V. Wintgens
Laboratoire de Recherche sur les Polymères
2–8 rue Henri Dunant, 94320 Thiais (France)

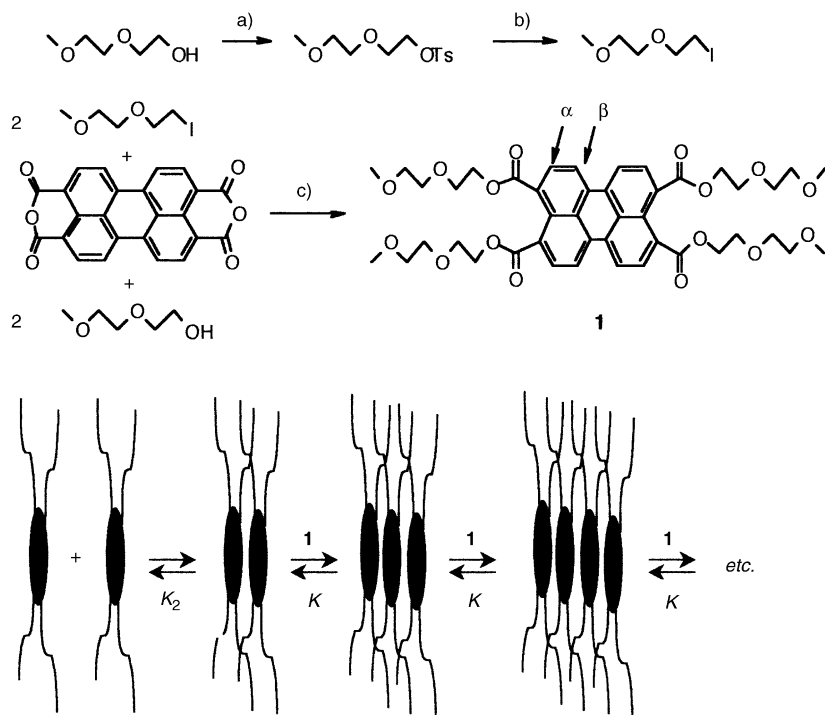
Dr. F. Boué, Dr. G. Carrot
Laboratoire Léon Brillouin
CEA-Saclay, 91191 Gif-sur-Yvette Cedex (France)

[**] Dr. Muriel Delepierre from the Unité de Résonance Magnétique Nucléaire des Biomolécules at the Pasteur Institut (Paris, France) is acknowledged for the high-dilution NMR measurements.



Supporting information for this article is available on the WWW under <http://www.angewandte.org> or from the author.

The hydrophobic aromatic core is derived from 3,4,9,10-perylenetetracarboxylic dianhydride (PTCA, Scheme 1), and treatment with an excess of (methoxyethoxy)ethyl iodide and (methoxyethoxy)ethanol, as adapted from a literature



Scheme 1. Synthesis and association of **1**. a) $\text{CH}_3\text{C}_6\text{H}_4\text{SO}_2\text{Cl}/\text{NaOH}/\text{water}/\text{THF}$, 0–5 °C, 96%; b) $\text{NaI}/\text{acetone}$, RT, 73%; c) K_2CO_3 , 70 °C, 47%. Ts = toluene-4-sulfonyl.

method,^[8] affords **1** as an orange wax (47% yield, not optimized). Extensive molecular analysis is in full agreement with the structure shown (see the Supporting Information).

Compound **1** does not aggregate in chloroform, as concluded from the concentration independence of the absorption and fluorescence spectra (data not shown). However, in more polar solvents, such as ethanol and water, the UV spectra are shifted and their resolution decline with the polarity of the solvent (Figure 1). This phenomenon is

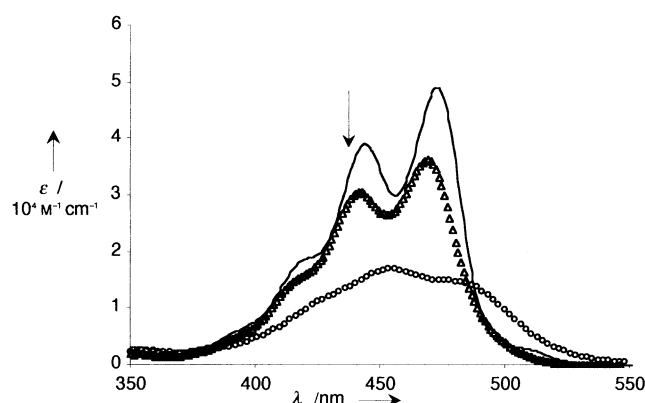


Figure 1. Normalized UV/Vis spectra of solutions of **1** (10^{-4} M) in several solvents. The arrows indicate the direction of change with increasing solvent polarity (—: chloroform, Δ : ethanol, \circ : water).

maximized in water, as expected. Figure 2 illustrates there is a clear dependence of the fluorescence spectra obtained in water on the concentration: the band at 480 nm, which can be assigned to the free monomer, disappears and a broader red-shifted band appears when the concentration is increased. These results indicate that self-assembly of **1** occurs in water.

A ^1H NMR spectroscopic analysis is in total agreement with these observations. Spectra of compound **1** (at $10^{-2} \text{ mol L}^{-1}$) are well-resolved in deuterated DMSO and chloroform; however, an upfield shift and a large broadening of the aromatic signals are observed at the same concentration in deuterated methanol. This phenomenon is probably related to self-association through aromatic stacking. The effect is even more pronounced in water as demonstrated in the NMR spectra obtained of **1** at increasing concentrations in deuterated water (see the Supporting Information). The inner protons (β) are most affected by the self-association: their chemical shifts vary from $\delta^\beta = 7.76$ ppm at $1.4 \times 10^{-6} \text{ M}$ to 5.81 ppm at $5.0 \times 10^{-2} \text{ M}$ (Figure 3).

The relative viscosity of aqueous solutions also increases with increasing concentration of **1** (see the Supporting Information). This observation agrees with a typical polymeric behavior of **1** in water on a macroscopic scale.

Compound **1** was designed to self-assemble in water in one-dimensional columns by π - π cofacial overlap and hydrophobic interactions. This model had already been proposed but not proved for the self-assembly of similar perylene derivatives in chloroform.^[9] We studied solutions of **1** in deuterated water at 25 °C using small-angle neutron scattering (SANS) to demonstrate that the expected monomolecular column structure forms in water. Figure 4 shows the product of the intensity I and the

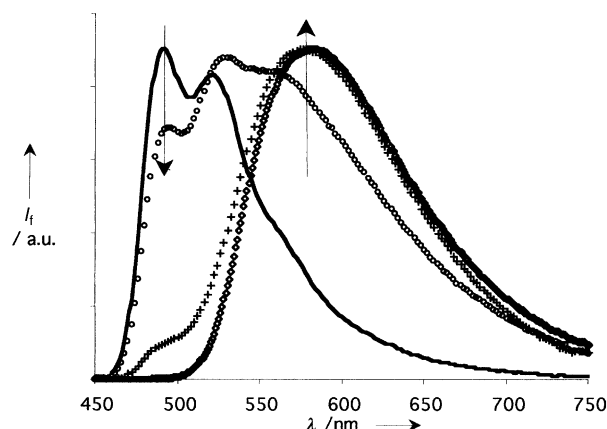


Figure 2. Fluorescence spectra of **1** in water, at 25 °C (—: $4 \times 10^{-7} \text{ M}$, \circ : 10^{-5} M , $+$: 10^{-4} M , \diamond : 10^{-2} M). Excitation wavelength: 425 nm. The arrows indicate the direction of change with increasing concentration.

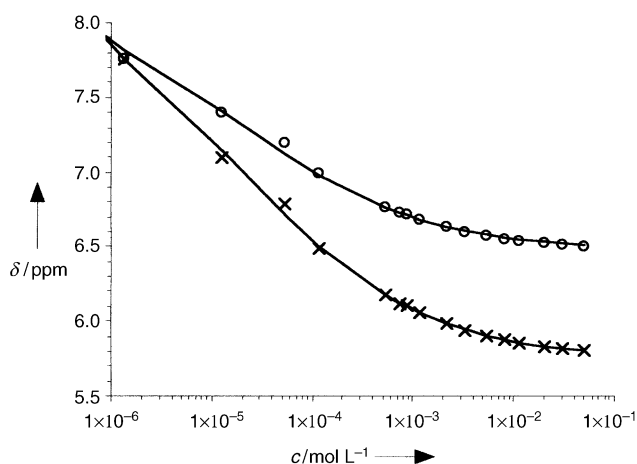


Figure 3. ^1H NMR chemical shifts of **1** in D_2O at 25°C versus concentration. \circ : aromatic protons α ; \times : aromatic protons β (see Scheme 1). Curves were calculated according to Equation (5), with the values of the association constants reported in Table 1 and $\delta_1^\beta = 9.27$ ppm, $\delta_i^\beta = 5.76$ ppm, $\delta_1^\alpha = 8.19$ ppm, and $\delta_i^\alpha = 6.47$ ppm.

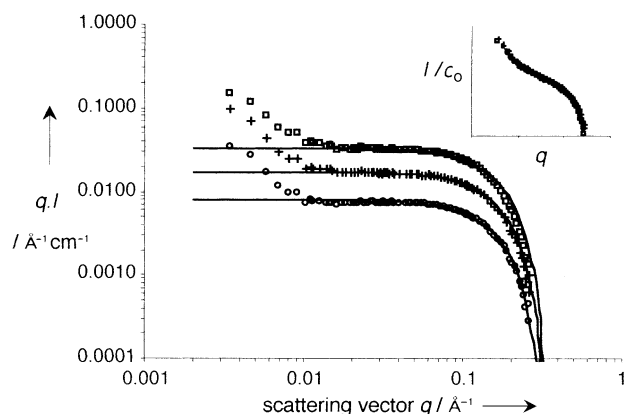


Figure 4. SANS data for solutions of compound **1** in D_2O at 0.5% (\circ), 1% ($+$), and 2% (\square) at 25°C . Curves were fitted according to Equation (1). Insert: I/c_0 versus q for the three concentrations.

scattering vector q versus q for three concentrations in a log-log plot. The insert shows that the scattered intensity is proportional to the concentration for the three concentrations studied. Therefore, it is reasonable to assume that no interobject interactions occur: the signal is proportional to the signal of one single object in this q range. The qI product at intermediate scattering vectors is constant and illustrates there is a q^{-1} dependence; this feature is a well-known characteristic of rodlike objects. However, the qI product increases when q tends towards zero, thus showing there is a stronger dependence of q on I . This result is attributed to the formation of larger additional aggregates.

A model of infinite rigid rods with circular cross-sections and a uniform scattering length density profile was used to describe the results.^[10] Fitting the scattering curves to Equations (1) and (2) provides the characteristics of the fibrillar objects:

$$I = \frac{\pi c}{q} \Delta b^2 M_L \left[2 \frac{J_1(qr)}{qr} \right]^2 \quad (1)$$

$$(qI)_{q \rightarrow 0} = (qI)_0 \exp\left(-\frac{r^2 q^2}{4}\right) \quad (2)$$

c is the rod concentration (g cm^{-3}), M_L is the mass per unit length of the rod (g Å^{-1}), Δb is its specific contrast (that is, the difference in the density of the scattering length between **1** and the solvent D_2O), r is the radius of the cross-section, and J_1 is the Bessel function of the first kind.

Figure 4 shows satisfying fits for $q \geq 0.01 \text{ Å}^{-1}$, thus establishing there is a constant rod diameter ($2r = 24 \text{ Å}$) over this concentration range. A 24-Å diameter corresponds to the largest dimension of compound **1** (29 Å , estimated with Chem3D software), which confirms that the rod is a one-dimensional assembly of stacked molecules of **1**, that is, a supramolecular polymer of monomer **1** in water.

A model involving an infinite number of equilibria (Scheme 1) can be used to describe the formation of long supramolecular chains. It is reasonable to suppose that the association constant is not influenced by the length of oligomers larger than dimers.^[11] The concentration of the free monomer (M_1) can be numerically calculated from the mass balance equation [Eq. (3)]:

$$c_0 = M_1 \left(1 + \frac{K_2}{K} \left(\frac{1}{(1 - K M_1)^2} - 1 \right) \right) \quad (3)$$

where c_0 is the total concentration and K_2 and K are the dimerization and multimerization constants, respectively. These association constants were determined by NMR and fluorescence spectroscopy.

The upfield shift of the aromatic protons was monitored over a wide concentration range by ^1H NMR spectroscopy ($c_0 = 10^{-6}$ – 10^{-1} M , Figure 3). In the stacking model we assign $f_1(\delta_1)$, $f_e(\delta_e)$, and $f_i(\delta_i)$ as the mole fractions (and the chemical shifts) of free monomer, molecules at the ends of the stack, and molecules within a stack, respectively. Moreover, we assume that $\delta_e = (\delta_1 + \delta_i)/2$.^[11] The observed chemical shift is then given by Equation (4):

$$\delta = f_1 \delta_1 + f_e (\delta_1 + \delta_i)/2 + f_i \delta_i \quad (4)$$

According to the two-constant model, and after some mathematical manipulations, we can derive Equation (5):

$$\delta = \frac{M_1}{c_0} \delta_1 + 2 \frac{K_2 M_1^2}{c_0 (1 - K M_1)^2} \frac{(\delta_1 + \delta_i)}{2} + \frac{K_2 K M_1^3}{c_0 (1 - K M_1)^2} \delta_i \quad (5)$$

In addition, we monitored the intensity of the band at 480 nm (normalized by the concentration, I_{480}) by fluorescence spectroscopy and determined the fraction of free monomer present in highly dilute solutions ($c_0 = 10^{-8}$ – 10^{-5} M) by using Equation (6).

$$f_1 = I_{480}/I_0 \quad (6)$$

I_0 is the normalized fluorescence intensity of the monomer (see the Supporting Information for more details).

We then fitted the experimental chemical shifts (δ) of the aromatic protons and the experimental values of f_1 (determined by fluorescence measurements) with Equations (5) and (6), respectively. The six adjustable parameters were K_2 , K , δ_1^a , δ_i^a , δ_1^b , and δ_i^b . The satisfactory fitting curves are shown in Figures 3 and 5, with the determined constants listed in Table 1.

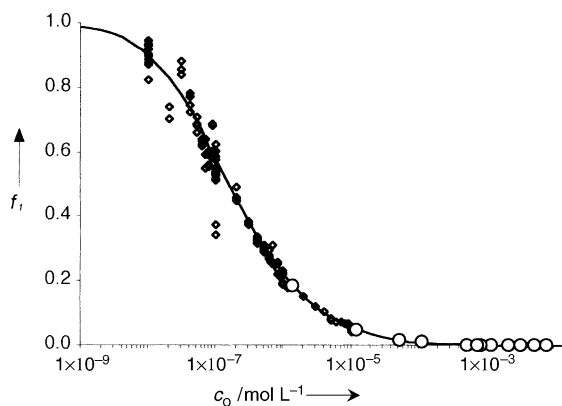


Figure 5. Fraction of free monomer **1** (f_1) versus concentration in water at 25 °C. The experimental fluorescence (\diamond) and NMR (\circ) data were fitted simultaneously with a two-constant model (—). The values of the constants are reported in Table 1.

Table 1: Characteristics of association of monomer **1** in water at room temperature.

$K_2^{[a]}$	$K^{[a]}$	$K/K_2^{[b]}$	$K^2/K_2^{[c]}$
$6(\pm 1.5) \times 10^6$	$8(\pm 1) \times 10^5$	0.13 ± 0.03	$1(\pm 0.1) \times 10^5$

[a] Dimerization (K_2) and multimerization (K) constants in L mol^{-1} .

[b] Measure of the cooperativity along the supramolecular chain.

[c] Association constant between oligomers in L mol^{-1} .^[12]

The large K_2 value illustrates the importance of the hydrophobicity of **1**. Unfortunately, the low K/K_2 value demonstrates an anticooperative association process: oligomerization is disfavored over dimerization. This anticooperativity could be the result of electronic effects and/or the steric bulk of the hydrophilic side chains. The association constant between two oligomers ($K^2/K_2 = 10^5 \text{ L mol}^{-1}$) can be considered as the most relevant parameter for the strength of the association.^[12] Knowledge of the association constants makes it possible to compute the degree of polymerization of the supramolecular polymer versus concentration (see the Supporting Information). For example, the number average degree of polymerization (DP_n) at a concentration of 20 g L^{-1} is $\text{DP}_n = 60$. This significant, but modest, value is in agreement with the viscosity measured (see Supporting Information).

In summary, we have described the facile synthesis of an amphiphilic monomer and its ability to self-associate. Investigations of both the structure and the strength of these assemblies have shown that the design of the monomer is well-suited for self-association in polar and protic solvents,

especially in water. These assemblies are long monomolecular wires, that is, aqueous supramolecular polymers. However, the association exhibits an anticooperative feature, which unfortunately limits the material properties of the resulting polymer at present. Therefore, improving the association strength is the next stage.

Experimental Section

Synthesis: see the Supporting Information.

Self-assembly: Measurements of the self-association were recorded on a Bruker ARX 500 MHz instrument, and very dilute solutions (10^{-5} M and 10^{-6} M) were analyzed on a Varian 600 MHz Innova spectrometer with a cryoprobe. UV/Vis spectra were recorded on a Varian Cary 1G spectrometer and fluorescence measurements were carried out on a LSM Aminco 8100 fluorimeter (LRP, Thiais, France). SANS experiments were performed on PACE and PAXY instruments at the LLB (Saclay, France).

Received: December 1, 2003 [Z53434]

Keywords: arenes · π interactions · polymers · self-assembly · supramolecular chemistry

- [1] a) N. Zimmerman, J. S. Moore, S. C. Zimmerman, *Chem. Ind.* **1998**, 604–610; b) *Supramolecular polymers* (Ed.: A. Ciferri), Marcel Dekker, New York, **2000**; c) L. Brunsveld, B. J. B. Folmer, E. W. Meijer, R. P. Sijbesma, *Chem. Rev.* **2001**, *101*, 4071–4097; d) A. Ciferri, *J. Macromol. Sci. Polym. Rev.* **2003**, *43*, 271–322.
- [2] R. P. Sijbesma, F. H. Beijer, L. Brunsveld, B. J. B. Folmer, J. H. K. K. Hirschberg, R. F. M. Lange, J. K. L. Lowe, E. W. Meijer, *Science* **1997**, *278*, 1601–1604.
- [3] F. Lortie, S. Boileau, L. Bouteiller, C. Chassenieux, B. Demé, G. Ducouret, M. Jalabert, F. Lauprêtre, P. Terech, *Langmuir* **2002**, *18*, 7218–7222.
- [4] a) L. Brunsveld, J. A. J. M. Vekemans, B. G. G. Lohmeijer, E. W. Meijer, *Chem. Commun.* **2000**, 2305–2306; b) L. Brunsveld, J. A. J. M. Vekemans, J. H. K. K. Hirschberg, R. P. Sijbesma, E. W. Meijer, *Proc. Natl. Acad. Sci. USA* **2002**, *99*, 4977–4982.
- [5] A. Harada, Y. Kawaguchi, T. Hoshino, *J. Inclusion Phenom. Macrocyclic Chem.* **2001**, *41*, 115–121.
- [6] N. Boden, R. J. Bushby, C. Hardy, F. Sixl, *Chem. Phys. Lett.* **1986**, *123*, 359–364.
- [7] J. H. Fuhrhop, C. Demoulin, C. Boettcher, J. König, U. Siggel, *J. Am. Chem. Soc.* **1992**, *114*, 4159–4165.
- [8] I. Seguy, P. Jolinat, P. Destruel, R. Mamy, H. Allouchi, C. Courseille, M. Cotrait, H. Block, *ChemPhysChem* **2001**, *2*, 448–452.
- [9] W. Wang, J. J. Han, L. Q. Wang, L. S. Li, W. J. Shaw, A. D. Q. Li, *Nano Lett.* **2003**, *3*, 455–458.
- [10] P. Terech, A. Coutin, *Langmuir* **1999**, *15*, 5513–5525.
- [11] R. B. Martin, *Chem. Rev.* **1996**, *96*, 3043–3064.
- [12] V. Simic, L. Bouteiller, M. Jalabert, *J. Am. Chem. Soc.* **2003**, *125*, 13148–13154.